

Optimisation of significant parameters through response surface methodology in the synthesis of silver nanoparticles by chemical reduction method

Mina Ahani, Marziyeh Khatibzadeh ✉

Department of Polymer Engineering and Color Technology, Amirkabir University of Technology, Tehran 15875-4413, Iran

✉ E-mail: khatib@aut.ac.ir

Published in Micro & Nano Letters; Received on 20th April 2017; Accepted on 11th May 2017

Response surface methodology coupled with the central composite design (CCD) was employed to optimise the significant parameters in the synthesis of silver nanoparticles (AgNPs) by chemical reduction method to obtain smaller average particle size. Different parameters such as the ethylene glycol (EG) concentration as reducing agent, the polyvinyl pyrrolidone (PVP) content as stabiliser and the pH were selected as they have the dominant effects on the particle size of AgNPs. Each of these parameters was studied at three levels. The average particle size of AgNPs was considered as the response value and determined by dynamic light scattering (DLS) analysis. The statistical analysis showed that the pH emerged as the most significant parameter influencing the average particle size and after that, the PVP content was also a significant parameter. The AgNPs synthesised under optimal conditions (6.88 M of EG, 0.5% of PVP and pH = 11) were characterised by UV-vis spectroscopy, X-ray diffraction (XRD), DLS, zeta potential, field emission scanning electron microscope and energy dispersive X-ray analysis. The XRD pattern showed the face-centred cubic silver and the average crystallite size of AgNPs was 30 nm. The average particle size of AgNPs was 37.35 nm according to DLS analysis, which was in good agreement with the predicted value (37.65 nm) by CCD.

1. Introduction: Silver nanoparticles (AgNPs) are clusters of silver atoms having the diameter in the range of 1–100 nm. They have been attracting interest due to their excellent optical, electrical, thermal, antimicrobial and localised surface plasmon resonance properties [1–3]. These nanoparticles (NPs) are already finding applications in a wide variety of fields including printed electronic devices [4], plasmonics [5], antibacterial materials [6] and biosensors [7]. Among these applications, printed electronic devices have gained considerable interest in recent years [8]. The conductive ink is the main core of these devices and AgNPs are an alternative for preparation of these inks due to their relatively low cost, high conductivity and good stability in ambient conditions [9]. Generally, after printing a conductive ink onto a substrate, it is thermally sintered at temperatures above 100°C. Then, a continuous conductive thin film forms upon solvent evaporation. Sintering is the last and necessary stage to obtain the electrical contact between NPs [10]. This high sintering temperature is not usually compatible with the common polymer substrates, such as polyethylene terephthalate (PET) or polycarbonate (PC), which have relatively low glass transition temperatures (T_g). Thus, the development of a sintering process at a lower temperature is required for application on polymeric substrates [11]. On the other hand, since the melting points of metal particles fall drastically with reducing the particle size [12], it would thus be possible to significantly lower the sintering temperature of AgNPs by reducing the particle size. Therefore, it is very important to synthesise AgNPs with smaller sizes for application in conductive ink.

Several techniques have been employed to synthesise AgNPs, such as physical [13], chemical [14, 15], photoreduction [16], sol-gel [17], microemulsion [18], sonochemical [19] and electrochemistry [20] methods. Among these various techniques, the chemical reduction method due to its simplicity, low cost and ability to produce large quantities is probably the most popular one. This method involves the reduction of silver salt using a reducing agent in the presence of a suitable stabiliser to prevent the aggregation of AgNPs [14]. In this method, the various parameters such as silver salt concentration, reducing agent concentration, stabiliser content, temperature, pH and reaction time influence the properties of AgNPs [15]. Most of the studies show that the optimisation of these parameters is usually carried out by changing a

single parameter while keeping all the other parameters fixed at a specific set of conditions. This procedure requires a huge number of necessary experiments with increasing time, cost and consumption of reagents. Also, this procedure is inefficient for providing enough information to study interrelationships between parameters [21]. To overcome this problem, statistical experimental design such as response surface methodology (RSM) has been suggested to determine the effects of parameters and their interactions. RSM is a popular and widely used technique for developing, improving and optimising the process and can be used to evaluate the significance of affecting parameters and their interactions [22]. The main objective of RSM is determining the optimal conditions for the system. It uses an experimental design such as the central composite design (CCD) to fit a polynomial equation to the experimental data to describe the behaviour of parameters. Adequacy of the applied model is then obtained by analysis of variance (ANOVA). The response surface plots can be applied to study the surfaces and locate the optimal conditions [23].

This study is a novel approach involving the optimisation of significant parameters in synthesis of AgNPs by chemical reduction method using statistical experimental design. First of all, three parameters are selected including the ethylene glycol (EG) concentration, the polyvinyl pyrrolidone (PVP) content and the pH that can be affected in the particle size of AgNPs. Then, a central composite experimental design is used to determine optimal synthesis conditions in order to yield AgNPs with small particle size in a simple and cost-effective way by reduction of aqueous solution of silver nitrate. Accordingly, the optimal synthesis conditions have been obtained and the synthesised AgNPs under these conditions are characterised by various methods, such as UV-vis spectroscopy, X-ray diffraction (XRD), dynamic light scattering (DLS), zeta potential, field emission scanning electron microscope (FE-SEM) and energy dispersive X-ray (EDX).

2. Experimental

2.1. Chemicals and synthesis of AgNPs: AgNPs were synthesised using silver nitrate (AgNO_3 , purity 99.9%) as an Ag precursor, ethylene glycol ($\text{C}_2\text{H}_6\text{O}_2$) as a reducing agent, polyvinylpyrrolidone ($\text{C}_6\text{H}_9\text{NO}$)_n as a stabiliser and sodium hydroxide as a pH regulator. These materials were all purchased from Merck

Chemicals, Germany and used without further purification. All of the solutions were prepared using deionised (DI) water purchased from Zolal Company, Iran.

To produce the AgNPs, an aqueous solution of 5 mM silver nitrate set on a magnetic stirrer plate. Then, the solution of PVP at a given concentration was added to a silver nitrate solution and allowed to stir constantly. After stirring for 10 min, the solution of EG at a certain concentration was added and 1 M solution of sodium hydroxide was used to adjust the pH. After the addition of reducing agent, the colour of the solution changed from colourless to light yellow and finally to dark brown, indicating the formation of AgNPs. The whole mixture was vigorously stirred at room temperature for 30 min.

2.2. Characterisation techniques: The absorption spectra of AgNPs solution at different reaction conditions were immediately measured in the range of 300–800 nm with a 1 nm resolution at room temperature, using a UV–vis spectrometer (JENWAY-6715, UK) with DI water as a reference.

Resulting AgNPs solution was centrifuged at 9000 rpm for 30 min. The solid residues of AgNPs were washed twice with DI water and then redissolved in absolute ethanol. Finally, it was dried by evaporating at 80°C to obtain the powder of the samples for XRD measurements. The XRD analysis was conducted by a Bruker AXS: D8 ADVANCE diffractometer, using monochromatic Cu α radiation ($\lambda = 1.5406 \text{ \AA}$) operated at a voltage of 40 kV and 30 mA current in the 2θ range of 5°–80°.

The size distribution and stability of AgNPs in the colloids were determined by DLS technique and zeta potential using a Zetasizer Nano ZS system (Malvern Instruments) applying a 660 nm laser oriented at 90° relative to the sample. Measurement parameters were as follows: measurement temperature of 25°C, a medium viscosity of 0.8872 mPa s and a medium refractive index of 1.330 and material refractive index of 0.15.

FE-SEM (FE-SEM, Mira TESCAN) was used to visualise the morphology and shape of NPs with an acceleration voltage of 15 kV. Samples were prepared by depositing a drop of solution on an aluminium grid sample holder and dried at room temperature. Then, they were coated with a thin layer of gold using a sputter coater (EMITECH K450X, England) prior to measuring by FE-SEM. EDX analysis was performed on a SUPRA55 (CARL ZEISS, Germany) coupled to the FE-SEM in order to confirm the presence of Ag crystals in the NPs.

2.3. Optimisation of experimental parameters: The statistical experimental design plays a main role in the methodology by making all influencing parameters changing simultaneously over a set of planned experiments so as to obtain the relation between these parameters and the output response of the studied process [24]. RSM is a collection of mathematical and statistical methods in analysing experiments based on the fit of a polynomial equation to the experimental data. This design procedure involves the steps as follows: (i) choosing independent variables of the main effects on the system; (ii) the selection of the experimental design and performing the experiments; (iii) the obtained experimental data processing; (iv) the evaluation of the model's fitness; and (v) obtaining the optimum values for each studied variable [21, 24].

As stated earlier, the statistical experimental design used here to optimise the three parameters, the EG concentration (A), the PVP content (B) and the pH (C). The predicted response was the average particle size. After determination of those independent variables, a CCD under RSM was employed to optimise the three parameters at three coded levels as shown in Table 1. The CCD contains a total of 20 experimental runs. The results of CCD experiments for studying the effect of three independent variables are presented along with obtained responses in Table 2.

Table 1 Used parameters and levels used in this experiment

Coded level	Parameters		
	A (EG concentration, M)	B (PVP content, %)	C (pH)
−1	3	0.2	7
0	6	0.6	9
1	9	1	11

Table 2 CCD experiments and obtained responses

Run no.	A	B	C	Average particle size, nm
1	9	1.0	11	46.11
2	3	1.0	7	94.00
3	6	0.6	9	67.00
4	6	0.6	9	67.88
5	9	0.2	11	41.00
6	6	0.6	7	86.50
7	9	0.2	7	92.22
8	6	0.6	9	67.50
9	9	0.6	9	70.30
10	9	1.0	7	95.40
11	3	0.6	9	69.00
12	6	0.6	11	40.00
13	6	0.6	9	66.00
14	3	1.0	11	48.50
15	3	0.2	11	43.00
16	6	0.6	9	67.50
17	6	0.2	9	71.14
18	6	1.0	9	76.17
19	6	0.6	9	67.32
20	3	0.2	7	93.65

Then, the obtained experimental data were analysed using Minitab® 16 software (Minitab, Inc., State College, PA, USA) and fitted to a second-order polynomial model as expressed in the following equation:

$$Y = \beta_0 + \beta_1 A + \beta_2 B + \beta_3 C + \beta_{11} A^2 + \beta_{22} B^2 + \beta_{33} C^2 + \beta_{12} AB + \beta_{13} AC + \beta_{23} BC \quad (1)$$

where Y is the dependent variable (average particle size of AgNPs); A , B and C are the coded independent variables; β_0 is the regression coefficient at centre point; β_1 , β_2 and β_3 are the linear coefficients; β_{11} , β_{22} and β_{33} are the quadratic coefficients; and β_{12} , β_{13} and β_{23} are the second-order interaction coefficients.

The developed model was evaluated using statistical analysis including analysis of variance (ANOVA), Fisher's F -test and P -value (probability). The quality of the fit polynomial model was expressed by the coefficient of determination, R^2 . A high R^2 value close to 1.0 confirms the accuracy of the applied model. Finally, one experiment was performed using the suggested optimum values to validate the development of the CCD model.

3. Results and discussion

3.1. Formation of AgNPs: The AgNPs were prepared by chemical reduction method in aqueous solution of silver nitrate using EG and PVP as reducing agent and stabiliser, respectively. After the synthesis, each sample was diluted 20 times and was characterised by UV–vis spectroscopy, which has proved to be a very useful technique for the analysis of NPs. The UV–vis spectra in Fig. 1 illustrate strong peaks at 400–450 nm in all

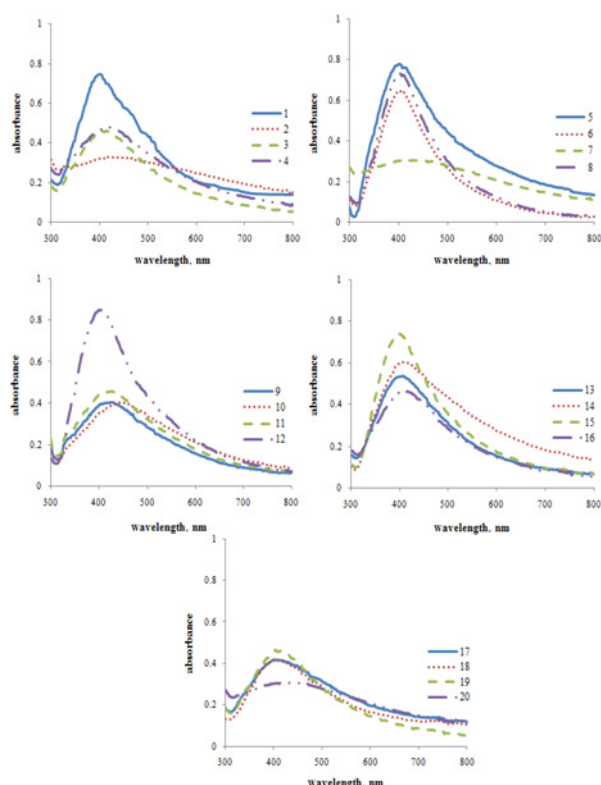


Fig. 1 UV-vis spectra of the AgNPs synthesised at different conditions

samples due to their surface plasmon resonance, which prove AgNPs formation [25].

3.2. CCD experiments and model fitting: The CCD pattern (Tables 1 and 2) was used to determine the optimal conditions and to select the parameters having a main influence on the particle size of AgNPs. Twenty experiments were performed to estimate the best conditions for the synthesis of AgNPs using the chemical reduction method. The structure of CCD and the results of measurements are presented in Table 2 and the smallest value of average particle size (40.00 nm) is shown in run no. 12. The samples were mainly characterised for their average particle size using DLS. For predicting the optimal conditions of AgNPs synthesis, a second-order polynomial model was fitted to the experimental results. The developed model was expressed as follows:

(see equation (2))

where the average particle size of AgNPs as yield (Y) was a function of EG concentration (A), PVP content (B) and pH (C). The plot of experimental values of average particle size versus those calculated from equation indicated a good fit, as presented in Fig. 2. The coefficient of determination (R^2) was calculated as 0.9986, indicating a good agreement between experimental and predicted values can explain up to 99.86% variability of the response.

ANOVA was employed to find the most important effects and interactions. ANOVA is a statistical technique for analysing experimental data. It subdivides the total variation in a set of data into

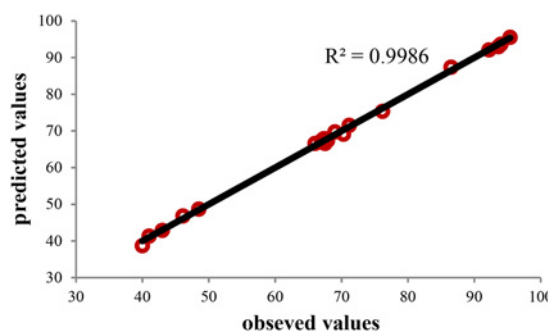


Fig. 2 Experimental data versus predicted data for average particle size of AgNPs

component parts associated with specific sources of variation for the model [26]. A P -value < 0.05 in the ANOVA table indicates the statistical significance of an effect at 95% confidence level. F -value was used to estimate the statistical significance of all parameters in the polynomial equation within 95% confidence interval. In general, the larger the magnitude of F , the smaller the value of P , the more significant is the corresponding coefficient term. The ANOVA response model of regression is represented in Table 3. ANOVA for AgNPs synthesis indicated that the ' F -value' of the model was 648.92, and the ' P -value' was < 0.0001 , suggesting that the model was statistically significant (Table 3). According to Table 3, it is observed that the coefficients for the linear parameters (B) and (C), the square parameters (A^2), (B^2) and (C^2) and the interaction parameter (BC) were highly significant on the basis of their P -values (< 0.05) whereas the linear parameter (A) and the interaction parameters (AB) and (AC) were insignificant to the response.

3.3. Response surface methodology: In the next step of the design, RSM was applied to give more detailed explanation for the influences of the three aforementioned independent variables and their interactive effects on the average particle size. Figs. 3a–c represent the three-dimensional (3D) response surface graphs and their corresponding contour plots (2D response surface plots) of the average particle size (nm) versus change in variables. These plots were obtained for a given pair of parameters at fixed and optimal values of other variables. In the contour plot, lines of the constant response are drawn in the plane of the independent variables. The contour plots help to visualise the shape of a response surface. When the contour plot displays ellipses or circles, the centre of the system refers to a point of maximum or minimum response. Sometimes, the contour plot may display hyperbolic or parabolic system of the contours. In this case, the stationary point is called a saddle point and it is neither a maximum nor a minimum point [27].

Fig. 3a shows the relative effects of two parameters, viz. EG concentration and PVP content on the average particle size when pH was kept at 11. It clearly exhibits a very strong degree of curvature of 3D surface and a fairly strong degree of curvature of 3D surface for PVP and EG, respectively, where the optimum level of two variables can be easily determined. It indicated that the average particle size decreased with the increase of the PVP content from 0.2 to 0.5% and thereafter rapidly increased with the increase of the PVP content from 0.5 to 1%. It also observed that the average particle size slightly decreased with the increase of the EG concentration from 3 to 6.88 M and thereafter increased with the increase of

$$\begin{aligned}
 Y \text{ (average particle size of AgNPs, nm)} = & 67.3142 - 0.3120A + 1.9170B - 24.3160C \\
 & + 1.5545A^2 + 5.5595B^2 - 4.8455C^2 \\
 & + 0.3050AB - 0.5450AC + 0.8850BC
 \end{aligned} \quad (2)$$

Table 3 ANOVA for CCD

Source of variation	Sum of squares	Degree of freedom	Mean square	F-value	P-value
model	6084.54	9	676.06	648.92	0.000
A	0.97	1	0.97	0.93	0.362
B	36.75	1	36.75	35.27	0.000
C	5912.68	1	5912.68	5675.29	0.000
A ²	15.45	1	6.49	6.23	0.037
B ²	46.28	1	82.96	79.63	0.000
C ²	63.02	1	63.02	60.49	0.000
AB	0.74	1	0.74	0.71	0.423
AC	2.38	1	2.38	2.28	0.169
BC	6.27	1	6.27	6.01	0.040
lack of fit	6.81	5	1.36	2.67	0.224
pure error	1.53	3	0.51		
total	6094.65	19			

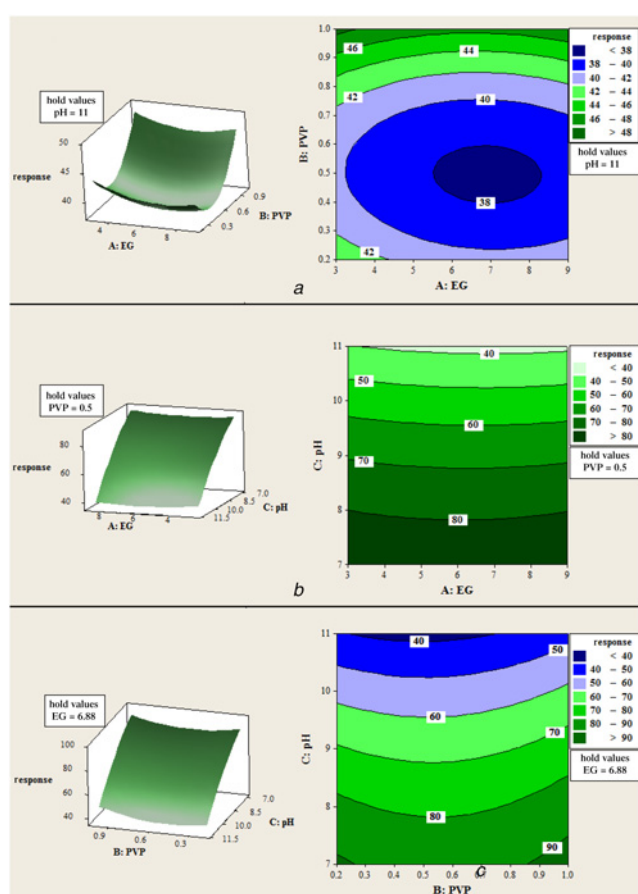


Fig. 3 Response surface graphs and its corresponding contour plots for average particle size of AgNPs as a function of
a EG concentration and PVP content at pH = 11
b EG concentration and pH at PVP = 0.5%
c PVP content and pH at EG = 6.88 M

the EG concentration from 6.88 to 9 M. The contour plot for Fig. 3a exhibited an elliptical nature and the optimal conditions are exactly located inside the design boundary. Fig. 3b shows the dependence of the average particle size on the EG concentration and pH at fixed PVP content of 0.5%. The decrease in average particle size at higher pH was observed and the minimum response can be achieved when EG concentration and pH at the value of 6.88 M and 11, respectively. The contour lines in the corresponding contour plot show very low curvature, implying that there was an insignificant

interactive effect on the average particle size between EG concentration and pH. In Fig. 3c, when the 3D response surface plot was developed for the average particle size with varying PVP content and pH at a fixed EG concentration of 6.88 M. It indicated that the minimum response can be achieved when PVP content and pH at the value of 0.5% and 11, respectively. The contour lines in the corresponding contour plot show a considerable curvature, implying that there was a significant interactive effect on the average particle size between PVP content and pH. These results implied that the EG concentration exerted a trifling impact on the average particle size whilst the PVP content and pH exerted a significant impact on it, as also confirmed by statistical ANOVA results. However, pH exhibited the most significant effect on the average particle size compared to two other variables as revealed by the large coefficient value (24.3160). The slanting lines of observed response in Fig. 3c also favoured the similar conclusion. It might be interpreted by the fact that higher pH led to an increase in the reduction rate of the precursor resulting in a smaller average particle size. It is for this reason that when AgNO₃ solution was mixed with NaOH solution first it will favour the formation a pure silver oxide (Ag₂O) and if a reducing agent (ethylene glycol) was also added, then the product became metallic Ag. Compared with silver ion (Ag⁺), silver oxide is very easily reduced to metallic Ag. So, at higher pH values, smaller average particle size is due to the formation of silver oxide and the higher reduction rate [28].

After pH, the PVP content was also a significant parameter. PVP acts as a stabiliser for the dissolved metallic salts through electrostatic and steric stabilisation of the amide groups of the pyrrolidine rings and the methylene groups, respectively. To investigate the role of PVP content in the synthesis of AgNPs, experiments in which the PVP content was adjusted from 0.2 to 1% (weight ratio of PVP to water) during the synthesis were performed. The results show that the PVP content significantly affects the average particle size of the resulting NPs. At low PVP content, the polymer cannot completely cover the Ag⁺ ions, and consequently agglomerated particles are produced. However, when the PVP content is increased to a maximum of 0.5%, well isolated NPs are obtained and the average particle size is reduced. With increasing PVP content from 0.5 to 1%, the more ions are covered by the polymer, which slows the reaction process down; as a result, the size of the NPs increases. The optimal PVP content in the reaction was found to be 0.5%. This PVP content provided the conditions required to fabricate AgNPs, whilst obtaining a NPs population with a sufficiently small average particle size.

The 2D illustrations of response surface function are shown in Fig. 4. In these plots, the response is plotted against each of the input variables while the other variables are held constant. The plot shows how the response changes with the variables over its range. From these prediction profilers, the optimal conditions for synthesis AgNPs with the smallest average particle size are predicted.

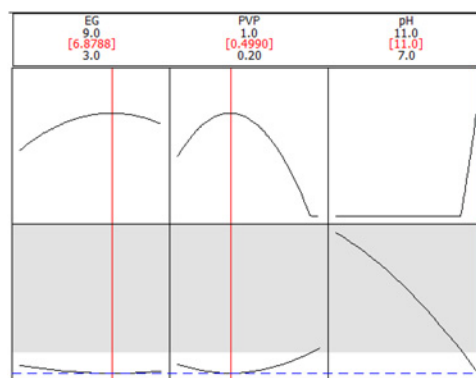


Fig. 4 Prediction profiler and optimal conditions for synthesis of AgNPs

From Fig. 4, it can be concluded that the optimal conditions giving the minimum response were found in conditions of $A = 6.88$ M, $B = 0.5\%$, $C = 11$ and at these conditions, the predicted value of Y (average particle size) was 37.65 nm.

3.4. Predictive model validation: To confirm the validity of the predicted model, a new experiment according to the optimal conditions was prepared. The observed optimal conditions show the average particle size of 37.35 nm, which was in good agreement with the predicted value (37.65 nm). A comparison between this observed result and theoretical prediction indicates the reliability of CCD used in optimising the synthesis of AgNPs, in terms of minimising the average particle size. The prepared AgNPs at optimal conditions was then subjected to characterisation examination.

3.5. Characterisation of AgNPs synthesised at optimal conditions: The UV-vis spectrum of AgNPs synthesised at optimal conditions is shown in Fig. 5. In this figure, a sharp peak is obtained at 399 nm. As mentioned in Section 3.1, this indicates the presence of AgNPs due to the excitation of surface plasmon resonance. The peak position in this sample compared with the 20 previous samples is shifted towards lower wavelength which indicates decrease in AgNPs size [29].

Fig. 6 shows the XRD pattern for optimised sample, which clearly indicates the formation of the silver crystalline structure. Four strong diffraction peaks at 38.32° , 44.52° , 64.69° and 77.67° can be attributed to the (111), (200), (220) and (311) crystal-line structures of the face centred cubic (FCC) silver, respectively (identified by ref: 01-087-0719). From Scherrer equation [29], the average crystallite size of 30 nm was determined for AgNPs. Whereas any peaks originating from silver oxides cannot be observed. However, one crystalline 'impurity' phase (star marks in Fig. 6) can also be identified from the pattern at a 2θ value of 32.37° and 46.41° , which are weaker than those of silver and corresponded to AgCl (identified by ref: 00-001-1013).

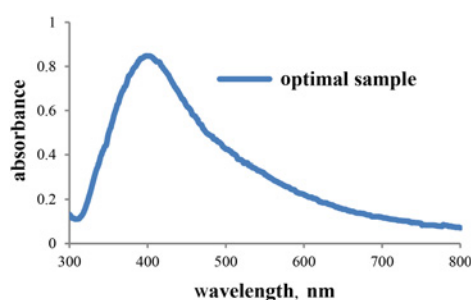


Fig. 5 UV-vis spectrum of the AgNPs synthesised at optimal conditions

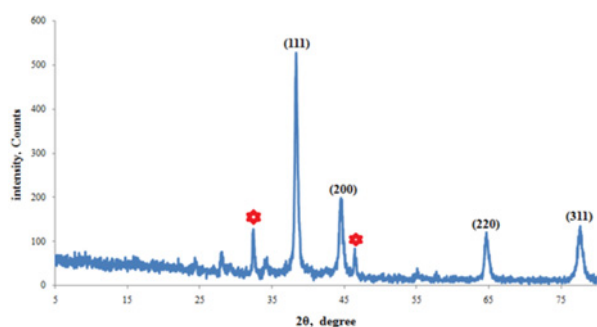


Fig. 6 XRD pattern of the AgNPs synthesised at optimal conditions

The particle size distribution image of the AgNPs synthesised at optimal conditions is shown in Fig. 7a. It is observed that the size distribution of AgNPs ranges from 10 to 60 nm. The calculated average particle size distribution of AgNPs is 37.35 nm. This result was in good agreement with the predicted value (37.65 nm) by CCD. The zeta potential of the AgNPs was found as a sharp peak at -22.80 mV (Fig. 7b). It is suggested that the surface of the NPs is negatively charged and dispersed in the medium. The negative value confirms the repulsion among the particles and proves that they are stable.

To analyse the results of DLS test for the optimised sample, FE-SEM images were studied. FE-SEM technique was used to visualise the morphology and shape of the NPs and also to confirm the size of the AgNPs. The FE-SEM images of the AgNPs for optimised sample are shown in Fig. 8. The surface morphology of NPs showed NPs are spherical in shape and the particle size ranges from 20 to 60 nm with narrow size distribution. This result was in good agreement with DLS result.

The synthesised AgNPs at optimal conditions were studied using EDX since the peaks obtained from the EDX spectrum give a clear idea about the elements present in the synthesised NPs. The EDX spectrum of the NPs in Fig. 9 shows a strong peak at 3 keV, which confirms the presence of an Ag element without oxide layer. Generally metallic AgNPs show a typical strong peak at 3 keV, due to surface plasmon resonance [29]. Other than this, weak peaks for N and O are observed, which may originate from the stabiliser that capped to the surface of the AgNPs. The spectrum obtained during EDX studies were used for carrying out the quantitative analysis. Quantitative analysis proved high silver contents

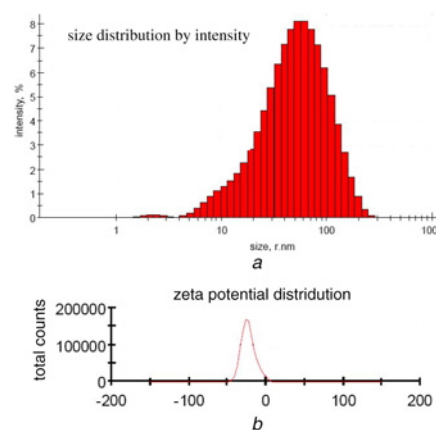


Fig. 7 Particle size distribution image
a DLS and
b Zeta potential of the AgNPs synthesised at optimal conditions

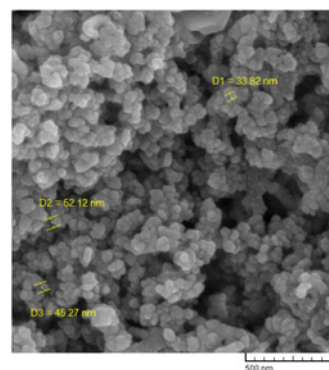


Fig. 8 FE-SEM images of the AgNPs synthesised at optimal conditions

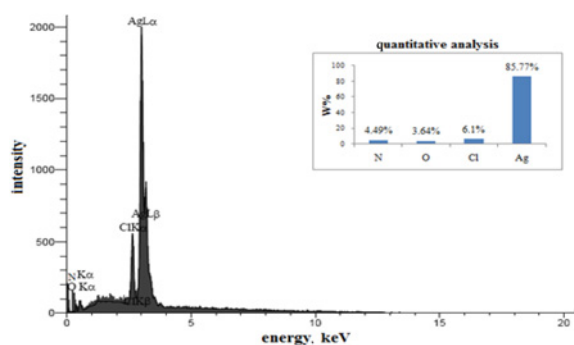


Fig. 9 EDX spectrum of the AgNPs synthesised at optimal conditions

(85.77%) in the sample. Except for Ag, we also show the presence of nitrogen, oxygen and chlorine the contents of which amounted to 4.49, 3.64 and 6.10%, respectively. The obtained results in the EDX spectrum were in accordance with the XRD results.

4. Conclusion: Our study serves as a novel approach as there are no published reports on the optimisation of significant parameters through statistical experimental design in the synthesis of AgNPs by reduction of silver nitrate with ethylene glycol as reducing agent and in the presence of PVP as a stabiliser. A CCD was used to optimise different parameters including reducing agent concentration, stabiliser content and pH for obtaining small average particle size. As a result, the pH and the PVP content were identified as the main parameters affecting the average particle size. The AgNPs synthesised under optimal conditions were characterised by UV-vis, XRD, DLS, zeta potential, FE-SEM and EDX analysis. The UV-vis spectrum confirmed the surface plasmon resonance of synthesised AgNPs. The XRD pattern showed the FCC Ag and the average crystallite size of AgNPs was 30 nm estimated from Scherrer method. The average particle size was obtained by DLS analysis and equal to 37.35, which was in good agreement with the predicted value (37.65 nm) by CCD. FE-SEM studies revealed spherical and uniform-shaped AgNPs with size in the range of 20–60 nm. Elemental analysis and particle stabilisation were determined by EDX and zeta potential techniques.

5 References

- [1] Lundahl P., Stokes R., Smith E., *ET AL.*: 'Synthesis and characterisation of monodispersed silver nanoparticles with controlled size ranges', *Micro Nano Lett.*, 2008, **3**, (2), pp. 62–65
- [2] Shenashen M.A., El-Safty S.A., Elshehy E.A.: 'Synthesis, morphological control, and properties of silver nanoparticles in potential applications', *Part. Part. Syst. Charact.*, 2014, **31**, pp. 293–316
- [3] Tian C., Mao B., Wang E., *ET AL.*: 'One-step, size-controllable synthesis of stable Ag nanoparticles', *Nanotechnology*, 2007, **18**, pp. 285607–285613
- [4] Perelaer J., Smith P.J., Mager D., *ET AL.*: 'Printed electronics: the challenges involved in printing devices, interconnects, and contacts based on inorganic materials', *J. Mater. Chem.*, 2010, **20**, pp. 8446–8453
- [5] Harra J., Mäkitalo J., Siikanen R., *ET AL.*: 'Size-controlled aerosol synthesis of silver nanoparticles for plasmonic materials', *J. Nanopart. Res.*, 2012, **14**, (6), pp. 870–879
- [6] Acharya D., Mohanta B., Pandey P., *ET AL.*: 'Optical and antibacterial properties of synthesised silver nanoparticles', *Micro Nano Lett.*, 2017, **12**, (4), pp. 223–226
- [7] Ma Y., Li N., Yang C., *ET AL.*: 'One-step synthesis of amino-dextran-protected gold and silver nanoparticles and its application in biosensors', *Anal. Bioanal. Chem.*, 2005, **382**, pp. 1044–1048
- [8] Yang W.D., Liu C.Y., Zhang Z.Y., *ET AL.*: 'One step synthesis of uniform organic silver ink drawing directly on paper substrates', *J. Mater. Chem.*, 2012, **22**, pp. 23012–23016
- [9] Yang W., Liu C., Zhang Z., *ET AL.*: 'Paper-based nanosilver conductive ink', *J. Mater. Sci. Mater. Electron.*, 2013, **24**, pp. 628–634
- [10] Greer J.R., Street R.A.: 'Thermal cure effects on electrical performance of nanoparticle silver inks', *Acta Mater.*, 2007, **55**, pp. 6345–6349
- [11] Perelaer J., Hendriks C.E., de Laat A.W., *ET AL.*: 'One-step inkjet printing of conductive silver tracks on polymer substrates', *Nanotechnology*, 2009, **20**, pp. 165303–165307
- [12] Huang Y., Risha G.A., Yang V., *ET AL.*: 'Effect of particle size on combustion of aluminum particle dust in air', *Combust. Flame*, 2009, **156**, pp. 5–13
- [13] Keskinen J., Ruuskanen P., Karttunen M., *ET AL.*: 'Synthesis of silver powder using a mechanochemical process', *Appl. Organomet. Chem.*, 2001, **15**, pp. 393–395
- [14] Lu Y.C., Chou K.S.: 'A simple and effective route for the synthesis of nano-silver colloidal dispersions', *J. Chin. Inst. Chem. Eng.*, 2008, **39**, pp. 673–678
- [15] Song K.C., Lee S.M., Park T.S., *ET AL.*: 'Preparation of colloidal silver nanoparticles by chemical reduction method', *Korean J. Chem. Eng.*, 2009, **26**, (1), pp. 153–155
- [16] Lu Y., Zhang C., Hao R., *ET AL.*: 'Morphological transformations of silver nanoparticles in seedless photochemical synthesis', *Mater. Res. Exp.*, 2016, **3**, (5), pp. 055014–055022
- [17] Epifani M., Giannini C., Tapfer L., *ET AL.*: 'Sol-gel synthesis and characterization of Ag and Au nanoparticles in SiO₂, TiO₂, and ZrO₂ thin films', *J. Am. Ceram. Soc.*, 2000, **83**, (10), pp. 2385–2393
- [18] Ray D., Chatterjee S., Sarkar K., *ET AL.*: 'Silver nanoparticles in hydrogels and microemulsions – a comparative account of their properties and bio-activity', *Mater. Res. Exp.*, 2014, **1**, (3), pp. 035022–035039
- [19] Darroudi M., Zak A.K., Muhamad M.R., *ET AL.*: 'Green synthesis of colloidal silver nanoparticles by sonochemical method', *Mater. Lett.*, 2012, **66**, pp. 117–120
- [20] Yin B., Ma H., Wang S., *ET AL.*: 'Electrochemical synthesis of silver nanoparticles under protection of poly(N-vinylpyrrolidone)', *J. Phys. Chem. B*, 2003, **107**, pp. 8898–8904
- [21] Marandi R., Khosravi M., Olya M.E., *ET AL.*: 'Photocatalytic degradation of an azo dye using immobilised TiO₂ nanoparticles on polyester support: central composite design approach', *Micro Nano Lett.*, 2011, **6**, (11), pp. 958–963
- [22] Balachandran M., Devanathan S., Muraleekrishnan R., *ET AL.*: 'Optimizing properties of nanoclay–nitrile rubber (NBR) composites using face centred central composite design', *Mater. Des.*, 2012, **35**, pp. 854–862
- [23] Ahmadi M., Vahabzadeh F., Bonakdarpour B., *ET AL.*: 'Application of the central composite design and response surface methodology to the advanced treatment of olive oil processing wastewater using Fenton's peroxidation', *J. Hazard. Mater. B*, 2005, **123**, pp. 187–195
- [24] Wu H., Yang R., Li R., *ET AL.*: 'Modeling and optimization of the flocculation processes for removal of cationic and anionic dyes from water by an amphoteric grafting chitosan-based flocculant using response surface methodology', *Environ. Sci. Pollut. R.*, 2015, **22**, pp. 13038–13048
- [25] Njagi E.C., Huang H., Stafford L., *ET AL.*: 'Biosynthesis of iron and silver nanoparticles at room temperature using aqueous sorghum bran extracts', *Langmuir*, 2011, **27**, (1), pp. 264–271
- [26] Nazari A., Mirjalili M., Nasirizadeh N., *ET AL.*: 'Optimization of nano TiO₂ pretreatment on free acid dyeing of wool using central composite design', *JIEC*, 2015, **21**, pp. 1068–1076
- [27] Sarlak N., Nejad M.A.F., Shakhesi S., *ET AL.*: 'Effects of electrospinning parameters on titanium dioxide nanofibers diameter and morphology: an investigation by Box–Wilson Central Composite Design (CCD)', *Chem. Eng. J.*, 2012, **210**, pp. 410–416
- [28] Chou K.S., Lu Y.C., Lee H.H.: 'Effect of alkaline ion on the mechanism and kinetics of chemical reduction of silver', *Mater. Chem. Phys.*, 2005, **94**, pp. 429–433
- [29] Anandalakshmi K., Venugobal J., Ramasamy V.: 'Characterization of silver nanoparticles by green synthesis method using *Petalium murex* leaf extract and their antibacterial activity', *Appl. Nanosci.*, 2016, **6**, pp. 399–408